Article

Dual-Core Mass-Balance Approach for Evaluating Mercury and ^{210}Pb Atmospheric Fallout and Focusing to Lakes

Peter C. Van Metre, and Christopher C. Fuller

Environ. Sci. Technol., **2009**, 43 (1), 26-32 • DOI: 10.1021/es801490c • Publication Date (Web): 02 December 2008

Environ. Sci. Technol. **2009,** *43,* 26–32

Dual-Core Mass-Balance Approach for Evaluating Mercury and ^{210}Pb Atmospheric Fallout and Focusing to Lakes

PETER C. VAN METRE*,† AND CHRISTOPHER C. FULLER‡

U.S. Geological Survey, 8027 Exchange Drive, Austin, Texas 78754, and U.S. Geological Survey, 345 Middlefield Rd., Menlo Park, California 94025

Received October 23, 2007. Revised manuscript received October 20, 2008. Accepted October 28, 2008.

Determining atmospheric deposition rates of mercury and other contaminants using lake sediment cores requires a quantitative understanding of sediment focusing. Here we present a novel approach that solves mass-balance equations for two cores algebraically to estimate contaminant contributions to sediment from direct atmospheric fallout and from watershed and in-lake focusing. The model is applied to excess ^{210}Pb and Hg in cores from Hobbs Lake, a high-altitude lake in Wyoming. Model results for excess ^{210}Pb are consistent with estimates of fallout and focusing factors computed using excess ^{210}Pb burdens in lake cores and soil cores from the watershed and model results for Hg fallout are consistent with fallout estimated using the soil-core-based ^{210}Pb focusing factors. The lake cores indicate small increases in mercury deposition beginning in the late 1800s and large increases after 1940, with the maximum at the tops of the cores of 16−20 μg/m^2•year. These results suggest that global Hg emissions and possibly regional emissions in the western United States are affecting the north-central Rocky Mountains. Hg fallout estimates are generally consistent with fallout reported from an ice core from the nearby Upper Fremont Glacier, but with several notable differences. The model might not work for lakes with complex geometries and multiple sediment inputs, but for lakes with simple geometries, like Hobbs, it can provide a quantitative approach for evaluating sediment focusing and estimating contaminant fallout.

Introduction

Atmospheric transport and deposition of contaminants has long been an important topic because the resulting contamination can be very widespread (*1*−*3*) and impact sensitive ecosystems and species (*4*). One of the most common approaches for evaluating atmospheric deposition rates and trends is to reconstruct fallout histories using lake sediment cores (*2, 5*−*7*). There are, however, complications in using lake cores to reconstruct deposition histories of atmospheric contaminants, including the effects of post-depositional migration and diagenesis, dating uncertainties, natural variability among sites (*3*), and sediment focusing (*5, 8*). Sediment focusing is the transfer of sediment and associated contaminants from other parts of the lake (*9, 10*) and, by some definitions, from the watershed (*11*) to the coring site. Because sediment focusing alters the contaminant accumulation rate at the coring site, it must be accounted for to use the core record to make an estimate of atmospheric deposition rate (*5, 12*).

One approach for evaluating sediment focusing is to use a fallout radionuclide, such as ^{137}Cs or ^{210}Pb, to calculate a focusing factor (FF) by comparing the core burden of the radionuclide with the measured or estimated fallout rate in the area. The radionuclide is assumed to trace the movement of sediments that accumulate atmospheric deposition. The FF is used to adjust core accumulation rates of contaminants to estimate their fallout rates (*12*−*16*). Other researchers have developed watershed delivery factors (e.g., the estimated fraction of fallout on the watershed delivered to the lake as a function of the drainage area to surface area (DA/SA) ratio) to account for focusing (*5, 17*).

The pathway of a contaminant to the lake can affect the relation between the concentration and mass flux of the contaminant in cores. If a contaminant is delivered to a lake primarily by direct atmospheric fallout on the lake and in-lake focusing is limited, contaminant concentrations for a given time interval will be inversely correlated among cores to the sediment mass accumulation rate (MAR): this can be described as a "fallout-dominated lake". In the ideal case, if sediment MAR in core 1 is twice the MAR in core 2, then concentrations of the contaminant for a given time horizon in core 1 will be half of those in core 2; contaminant mass flux will be equal, and equal to the fallout rate (Figure 1, parts a and b). The assumption of an inverse relation between concentration and MAR underlies the constant rate of supply (CRS) model for age dating cores using ^{210}Pb (*18*). If, on the other hand, the contaminant is delivered primarily by fluvial transport of particles from the watershed, then contaminant concentration profiles will be similar for multiple cores and mass flux will be proportional to sediment MAR (Figure 1, parts c and d); this can be described as a "fluvial input dominated lake". These contrasting scenarios were described by Eisenreich et al. (*19*) for cores from two sites in Lake Ontario for mirex (fluvial input dominates) and PCBs (fallout dominates). Most lakes fall somewhere between fallout and fluvial dominance, with the importance of fluvial inputs increasing with DA/SA ratio (*5*) and with watershed contaminant sources (e.g., urban land use) (*15*). Seepage lakes, with DA/SA ratios near 1, are more likely to approach the ideal fallout-dominated case (*20*), whereas urban reservoirs approach the ideal fluvial-dominated case (*21, 22*). Because in-lake focusing is particle-associated transport, it can lead to relations between concentration and MAR in cores like the fluvial-dominated case (Figure 1, parts c and d), even in small seepage lakes with no fluvial input from the watershed. These relations suggest that the comparison of contaminant concentrations and MARs in two or more cores from the same lake has the potential to indicate the relative amount of atmospheric input and particle-associated input of a contaminant to the cores.

The objective of the study presented here was to estimate atmospheric fallout and fluvial inputs of ^{210}Pb and Hg to a lake on the basis of relations between contaminant concentration, mass flux, and sediment MAR in two cores. Existing methods (*15, 16*) also were used to evaluate sediment focusing and to estimate fallout on the basis of ^{210}Pb inventories in lake cores and soil cores from the watershed.

* Corresponding author phone: (512) 927-3506; fax: (512) 927-3590; e-mail: pcvanmet@usgs.gov.
† Austin, Texas.
‡ Menlo Park, California.

10.1021/es801490c
Published on Web 12/02/2008

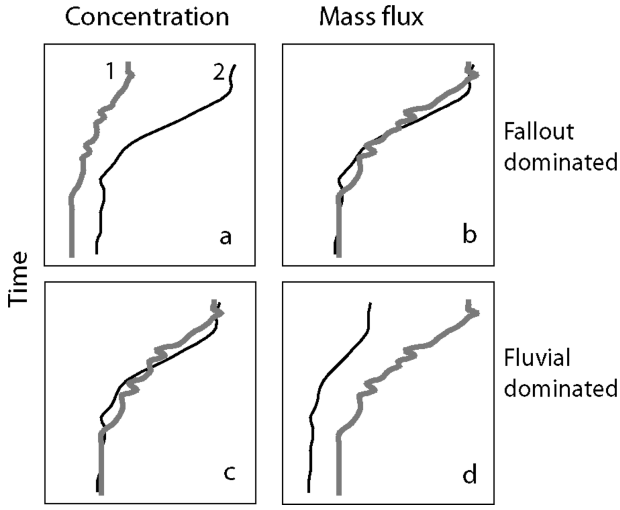

FIGURE 1. Conceptual relation between concentration and mass flux of a contaminant in two cores from the same lake where core 1 has a MAR twice that of core 2. In panels a and b, all contaminant input is by direct fallout, resulting in concentration enrichment in the low-MAR core (2) relative to the high-MAR core (1). In panels c and d, all input is of fluvial origin, resulting in similar concentrations and scaling of contaminant mass flux proportional to MAR.

Experimental Section

Hobbs Lake is at 3050 m elevation, 8 km west of the Continental Divide in the Wind River Range of the Rocky Mountains in west-central Wyoming (Supporting Information Figure S-1). The lake surface area is 0.084 km^2, and the drainage area is 3.59 km^2 (DA/SA ratio = 43). The watershed is underlain by granite, and there are numerous rock outcrops at the land surface. The lake is in the Bridger Wilderness, designated as a Primitive Area in 1931 and a Wilderness in 1964. No mechanized vehicles or sustained human activities are permitted in the Wilderness, and no mining or logging has occurred in the area of Hobbs Lake. The lake is elongated with two small influent streams entering from the SE and outflow exiting to the north. It is about 12 km from the Upper Fremont Glacier, where a detailed Hg fallout history was reported from glacial ice cores (*23*); the ice core locations are just east of the Continental Divide at approximately 4000 m elevation.

Five sediment cores were collected from Hobbs Lake in August 2003 for analysis of radionuclides, major and trace elements, and selected organic compounds. The lake bottom is relatively flat and uniform in depth; depth at the coring locations ranged from 11.9 to 16.8 m (Supporting Information Figure S-1). Cores were collected using a 14 cm square, 50 cm tall, custom-built box corer that provides undisturbed sediment cores of relatively large cross-sectional area (*24*) (Supporting Information Figure S-2). Two of the cores (HOB.DN, for down lake from the inflow, and HOB.UP for up lake closer to the influent stream) were sampled at fine resolution (0.5 cm intervals and, below 10 cm in HOB.UP, 1 cm intervals) and used in this analysis.

Five soil cores were collected from the watershed to provide estimates of ^{210}Pb fallout to the area (Supporting Information Figure S-3). Soil cores were collected by driving 5 cm diameter polycarbonate tubes about 20 cm into the ground, then slicing the recovered soil into 2 cm intervals.

Freeze-dried sediment and soil samples were analyzed for total ^{210}Pb and ^{226}Ra by γ spectrometry based on ASTM methods C 1402-98 and E 181-98, similar to methodology described by ref *25*. Excess ^{210}Pb was calculated as the difference between total ^{210}Pb activity and ^{226}Ra activity. Elemental concentrations were determined on a 0.2 g freeze-dried and ground sample digested on a hotplate using a mixture of hydrochloric−nitric−perchloric−hydrofluoric acids with analysis by inductively coupled plasma mass spectrometry. Samples for mercury analysis were digested with nitric acid and sodium dichromate in a closed Teflon vessel. The digest was mixed with air and a sodium chloride−hydroxylamine hydrochloride−sulfuric acid solution, and then Hg^{2+} was reduced to Hg^0 with stannous chloride in a continuous flow manifold. The mercury vapor was separated and measured using cold vapor atomic adsorption spectrometry (*26*). Quality assurance was provided by determining elemental concentrations for duplicate samples and a variety of soil, lake, and marine reference samples (*26*). Selected elemental concentrations and radionuclide activities are presented in the Supporting Information (Tables S-1 and S-2).

Dual-Core Mass-Balance Model

We developed an approach that uses two cores from a lake to separate contaminant contributions from fallout on the lake and particle-associated input from other parts of the lake and the watershed; we call this approach the dual-core mass-balance (DCMB) model. The input of a constituent to an interval of a sediment core can be described by

$$X_i = X_L + X_W + X_{Fn} + X_{Fa} \quad (1)$$

where X_i is mass of the constituent in core interval i, X_L is the mass delivered from other parts of the lake, X_W is the mass delivered from the watershed, X_{Fn} is the mass delivered by natural fallout onto the lake, and X_{Fa} is the mass delivered by anthropogenic fallout onto the lake.

Constituent concentration in a core interval (C_i) can be calculated by dividing X_i by the mass of sediment in the interval (M_i):

$$C_i = X_L/M_i + X_W/M_i + X_{Fn}/M_i + X_{Fa}/M_i \quad (2)$$

The terms in eq 2 can be expressed as constituent flux divided by sediment flux (MAR, g/m^2·year) to interval i:

$$C_i = F_L/\mathrm{MAR}_i + F_W/\mathrm{MAR}_i + F_n/\mathrm{MAR}_i + F_a/\mathrm{MAR}_i \quad (3)$$

where F_L and F_W are the flux from other parts of the lake and the watershed, and F_n and F_a are natural and anthropogenic fallout (μg/m^2·year); these terms result in units of concentration. There are two primary pathways that a contaminant can take to the core: atmospheric deposition, with insignificant particle mass associated, and particle-associated transport. In-lake focusing and fluvial inputs from the watershed are both the result of particle-associated flux to the coring site and, in practice, are indistinguishable; therefore, the first two terms in eq 3 were combined to represent all particle-associated flux (F_P) to the coring site. F_P/MAR_i is equal to the average initial contaminant concentration in sediment deposited at the coring site (C_P (μg/g)), prior to in situ enrichment by atmospheric fallout. Diagenetic changes to sediment and contaminant mass (e.g., loss of organic matter) are assumed to have a negligible effect on concentrations.

C_i and MAR_i are measured, leaving three unknowns: C_P, F_n, and F_a. Equation 3, with F_P/MAR represented by C_P was formulated for each of two cores, and the two equations were combined by difference:

$$C_{i,1} - C_{i,2} = (C_{P,i,1} - C_{P,i,2}) + (F_n/\mathrm{MAR}_{i,1} - F_n/\mathrm{MAR}_{i,2}) + (F_a/\mathrm{MAR}_{i,1} - F_a/\mathrm{MAR}_{i,2}) \quad (4)$$

Subscripts 1 and 2 indicate the two cores and the intervals in the cores are matched by deposition date.

For the situation where $F_a = 0$ (e.g., excess ^{210}Pb), and $C_{P,i,1}$ and $C_{P,i,2}$ are equal, we can solve for F_n by

$$F_{n,i} = (C_{i,1} - C_{i,2})/(1/\mathrm{MAR}_{i,1} - 1/\mathrm{MAR}_{i,2}) \quad (5)$$

and for C_P by

$$C_{P,i,1} = C_{i,1} - (F_n/\mathrm{MAR}_{i,1}) \quad (6)$$

If $C_{P,i,1}$ and $C_{P,i,2}$ are not equal but the difference (ΔC_P) can be estimated, a term can be added to eq 5 to form eq 7. An example of a nonzero ΔC_P is the physical sorting of sediment in the down-lake direction.

$$F_{n,i} = ((C_{i,1} - \Delta C_P) - C_{i,2})/(1/\mathrm{MAR}_{i,1} - 1/\mathrm{MAR}_{i,2}) \quad (7)$$

Applying eq 5 or 7 to excess ^{210}Pb we can calculate the DCMB model focus factor ($\mathrm{FF_{DCMB}}$) as the ratio of the mean flux of excess ^{210}Pb in the core (equal to the burden in the core times the decay constant (λ) 0.03114 year^{-1}) to modeled F_n. For an anthropogenic contaminant, given estimates of F_n, initial C_P, and ΔC_P, eq 4 can be rearranged and solved for F_a and C_P for each interval by

$$F_a = \{(C_{i,2} - (C_{i,1} - \Delta C_P)) + [(F_n/\mathrm{MAR}_{i,1}) - (F_n/\mathrm{MAR}_{i,2})]\}/(1/\mathrm{MAR}_{i,2} - 1/\mathrm{MAR}_{i,1}) \quad (8)$$

and

$$C_{P,i,j} = C_{i,j} - F_n/\mathrm{MAR}_{i,j} - F_a/\mathrm{MAR}_{i,j} \quad (9)$$

where j is a core. This approach was used to evaluate fallout rates and sediment focusing for excess ^{210}Pb and Hg in cores from Hobbs Lake.

Results

Age Dating and Sediment Focusing. Cores HOB.DN and HOB.UP were dated using ^{210}Pb by applying the CRS model (*18*). The near-linear decrease in ln excess ^{210}Pb in core HOB.UP (Supporting Information Figure S-4) indicates a near-constant sediment MAR. The CRS model was used to assign dates down to the 14−15 cm interval dated as 1849 resulting in a mean MAR (since 1849) of 153 g/m^2·year. The ln excess ^{210}Pb profile in core HOB.DN is not linear, indicating temporal variation in sediment MAR (Supporting Information Figure S-4). The CRS model was used to assign dates down to the 7−7.5 cm interval dated as 1834; MAR ranges from 25 g/m^2·year in 1954 to 80 g/m^2·year in 1870. Uncertainty in date and MAR estimates was estimated by propagating measurement uncertainties to calculate additive and multiplicative errors using an approach similar to ref *27* (Supporting Information). Uncertainty in dates is quite large prior to 1900 (Supporting Information Table S-4 and Figure S-4), exceeding the age difference between adjacent intervals from about 1900 and earlier. Uncertainty in MARs is proportionally even greater, about 50% of the modeled MAR in 1900; thus, CRS dates and MARs for core intervals older than 1900 were not used in the DCBM model.

Focusing was estimated independently from the DCMB model using excess ^{210}Pb lake core and soil core burdens. The excess ^{210}Pb burdens in the soil cores ranged from 22.3 to 73.5 dpm/cm^2. The soil core with the largest burden (soil core 5; Supporting Information Figure S-3) was from near granite outcrops and a rock hill; the burden in that core is about 2.5 times the mean of the other four cores and exceeds the burdens in both of the Hobbs Lake cores. We concluded that excess ^{210}Pb activities in soil core 5 were enhanced by runoff from the bare granite nearby and, therefore, the burden was not representative of direct fallout. The mean excess ^{210}Pb burden from the other four cores (29.7 ± 10.3 dpm/g·cm^2) indicates an atmospheric fallout rate of 0.92 ± 0.32 dpm/cm^2·year. The excess ^{210}Pb burden for each lake core (39.8 and 62.9 dpm/cm^2 for HOB.DN and HOB.UP) was divided by the mean soil core burden yielding soil-core-based FF ($\mathrm{FF_{SC}}$) of 1.4 ± 0.4 and 2.1 ± 0.6 for HOB.DN and HOB.UP, respectively.

DCMB Model of ^{210}Pb Fallout and FFs. The DCMB model was applied to excess ^{210}Pb profiles in the Hobbs Lake sediment cores to estimate fallout rate and FFs. ΔC_P for excess ^{210}Pb was assumed to be zero on the basis of similar pre-1850 concentrations of total Pb (mean of 16.3 ± 1.6 μg/g HOB.DN and 15.3 ± 1.2 μg/g HOB.UP) indicating little down-lake sorting for Pb. Excess ^{210}Pb is assumed to be only from fallout. Excess ^{210}Pb activities for each interval were decay-corrected to the time of deposition, and HOB.UP values were interpolated by deposition date to the intervals of HOB.DN to create a common set of time intervals. We then applied eqs 5 and 6. For the period of 1900−2003, the time-weighted mean fallout rate of ^{210}Pb from the DCMB model is 1.0 dpm/cm^2·year (±0.11 (standard deviation of modeled values)) (Supporting Information Table S-4), 9% greater than the rate of 0.92 dpm/cm^2·year estimated from soil cores. Pre-1900 core intervals produced highly variable results in the model, perhaps because of rapidly increasing uncertainties in age-dates and MARs using the CRS model, and therefore were not used.

The decay-corrected excess ^{210}Pb accumulation rate in each core interval, which is constant as a result of using the CRS model, is 1.24 dpm/cm^2·year at HOB.DN and 1.95 dpm/cm^2·year at HOB.UP. The DCMB-based FF ($\mathrm{FF_{DCMB}}$), the ratio of the core accumulation rate and the modeled fallout rate, is 1.2 and 1.9 for HOB.DN and HOB.UP, respectively.

Calculation of Focusing Factors Using ^{210}Pb Core Burdens. A different mass-balance model can be applied to excess ^{210}Pb data to estimate fallout and focusing independent from age dating. A mass balance for excess ^{210}Pb in a core can be written in terms of the core burden:

$$A_0 = F_n(1/\lambda) + C_A(\Sigma M) \quad (10)$$

where A_0 (dpm/cm^2) is the integrated burden of excess ^{210}Pb in the core (same term used in the CRS model), F_n (dpm/cm^2·year) is the ^{210}Pb fallout rate ($F_n(1/\lambda)$ equals the burden of excess ^{210}Pb supported by direct fallout), C_A (dpm/g) is the time-weighted mean activity of excess ^{210}Pb in sediment delivered to the coring site (focusing) over the time span of A_0, and ΣM (g/cm^2) is the mass of sediment in the core for the same interval as A_0. The product of C_A and ΣM is the burden of excess ^{210}Pb supported by focusing (in-lake and watershed) inputs.

Equation 10 was written for each core, combined by difference, and solved for C_A (F_n cancels). Using A_0 of 39.9 and 62.9 dpm/cm^2 and ΣM of 0.89 and 3.01 g/cm^2 for HOB.DN and HOB.UP, respectively, we calculate C_A of 10.8 dpm/g. Solving for $F_n(1/\lambda)$ using eq 10, we obtain 30.2 dpm/cm^2, equivalent to a fallout rate of 0.94 dpm/cm^2·year, and FFs of 1.3 and 2.1 for HOB.DN and HOB.UP, respectively. These values are similar to the soil core estimated fallout rate and $\mathrm{FF_{DCMB}}$ and $\mathrm{FF_{SC}}$. The C_A, ΣM, λ, and the top of core MAR for HOB.UP (179 g/m^2·year) were used to estimate a current particle input activity of 57 dpm/g by rearranging the equation for estimating MAR from the CRS model (*18*). The estimated current particle input activity is the weighted average of fluvial particle activity from the watershed and activity of redistributed particles from within the lake (focusing). Actual particle activities are unknown; however, the mean activity in the 0−2 cm intervals in the five soil cores (soil core 5 included as representative of variations in surface soil activities in the watershed) is 49 dpm/g.

Hg Fallout Recorded in Hobbs Lake Cores. Mercury concentrations in the Hobbs Lake cores increased substantially during the past century with larger increases in the down-lake than up-lake core (Figure 2a). Higher sedimenta-

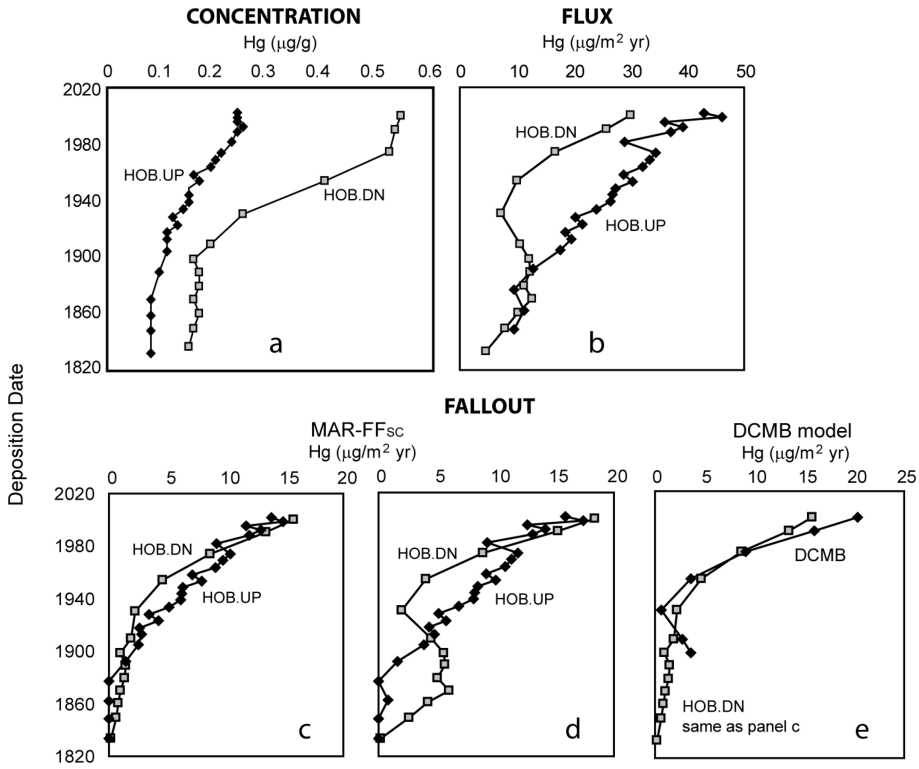

FIGURE 2. Profiles of mercury concentration (a), mass accumulation rate (b), and estimated anthropogenic fallout of mercury (c−e) in Hobbs Lake cores. Panels c−e are the following: (c) FF corrected using soil cores (MAR-FF_{SC}) with a background concentration correction, (d) MAR-FF_{SC} with a background flux correction, and (e) DCMB modeled fallout.

tion rate near the stream inflow suggests that lower Hg concentrations there result from greater dilution of atmospheric fallout by watershed sediment. Comparison of Hg flux in the cores (Figure 2b) indicates that Hobbs Lake is not a perfect fallout-dominated lake (Figure 1, parts a and b); if direct fallout where providing all of the Hg to the cores and there was no in-lake focusing, Hg fluxes would be equal. The greater sedimentation rate at HOB.UP more than compensates for the lower Hg concentrations relative to HOB.DN, resulting in greater total Hg flux.

Hg Fallout by the Focus-Corrected MAR Approach. Anthropogenic fallout of Hg to Hobbs Lake was estimated by a widely used focus-correction approach (*12, 15, 16*). The general steps are to correct Hg profiles for natural (background) Hg inputs then adjust corrected values for focusing by dividing by the FF. Two approaches were compared for background correction. The first subtracted background concentration from total Hg concentration to yield an "anthropogenic concentration". This approach assumes that background Hg is delivered to the cores primarily by particle-associated transport (focusing and watershed input). The background Hg concentrations at HOB.DN and HOB.UP, as indicated by pre-1850 values, are relatively stable with means of 0.14 and 0.077 μg/g, respectively. The higher background concentration at HOB.DN could be caused by sorting in the down-lake direction, by less dilution of natural fallout by sediment relative to HOB.UP, or by both. Anthropogenic concentrations were multiplied by sediment MAR to estimate the anthropogenic flux to each core interval. Anthropogenic flux was divided by FF_{SC} to estimate Hg fallout rate for each core (Supporting Information Table S-5, MAR-FF_{CC}). The resulting anthropogenic fallout profiles for the two cores are nearly identical (Figure 2c).

The second approach corrects for background inputs using flux. Mean pre-1850 concentration was multiplied by estimated pre-1850 MAR to yield background flux, which was subtracted from total Hg flux, then focus-corrected (Figure 2d; Supporting Information Table S-5, MAR-FF_{FC}). This approach assumes background Hg inputs are delivered primarily by direct fallout on the lake, pre-1850 MARs are reasonably known, and in-lake focusing and watershed inputs are limited. Unlike the concentration correction result (Figure 2c), this approach yields somewhat different results for the two cores with a modest increase in estimated mid-20th century fallout at HOB.UP and decrease at HOB.DN (Figure 2d). Natural Hg fluxes to the lake likely include direct fallout and particle-associated transport. The relatively stable pre-1850 concentrations (Supporting Information Table S-1) and similarity of MAR-FF_{CC} fallout estimates (Figure 2c) suggests particle-associated inputs might be greater.

Anthropogenic Hg fallout increases throughout the past century, with estimated deposition rates in 2000 of 13.9 and 15.8 $\mu g/m^2 \cdot$year (MAR-FF_{CC} fallout for HOB.UP and HOB.DN) and 15.9 and 18.3 $\mu g/m^2 \cdot$year (MAR-FF_{FC} fallout for HOB.UP and HOB.DN). The mean since the late 1990s for both cores and both background-correction approaches is 16.3 $\mu g/m^2 \cdot$year. The use of the FF_{DCMB} to focus correct results in about 12% higher fallout because of the smaller FFs. The increase in anthropogenic fallout during the 20th century results in total Hg flux ratios (top of core vs pre-1850s) of 4.6 and 6.5 for HOB.UP and HOB.DN, respectively.

Hg Fallout Using the DCMB Model. Measured Hg concentrations and sediment MARs in HOB.UP were interpolated to the intervals in HOB.DN by date to create a common set of values in time. Background F_n and C_P were estimated using eqs 6 and 7, mean Hg and organic carbon (OC) concentrations in pre-1850s samples, and mean MARs in the cores since 1890. The mean MAR was used for background estimates because of very large uncertainty in pre-1850 MAR. If ΔC_P is zero, application of eqs 6 and 7 results in F_n of 3.5 $\mu g/m^2 \cdot$year and background C_P of 0.056 μg/g. This F_n is similar to estimated preindustrial Hg fallout in Minnesota (3.7 $\mu g/m^2 \cdot$year) (*5*) but higher than from the Upper Fremont Glacier ice core (0.78 $\mu g/m^2 \cdot$year) (*23*). OC concentrations in background samples suggest down-lake sorting may play a role in higher Hg concentrations at HOB.DN; OC in back-

ground samples is about 20% larger in HOB.DN than in HOB.UP (means of 11.8% and 9.5%), and OC and Hg concentrations are strongly correlated ($r = 0.92$, $n = 14$). Correlation of Hg to OC transport has been demonstrated elsewhere (*28*). Down-lake sorting could result in relatively greater dilution of F_P at HOB.UP by preferential deposition of coarser clastic material that is lower in Hg, and/or in the enhanced transport of lighter and finer grained, carbon- and Hg-rich sediment down lake to HOB.DN. As presented above, ΔC_P for excess ^{210}Pb was assumed to be zero on the basis of similar background Pb concentrations in the cores; however, Pb geochemistry is different from Hg geochemistry in that Pb is strongly associated with particle surfaces (*29*) and not OC.

We estimated ΔC_P on the basis of equal carbon-normalized Hg concentrations in background sediments after enrichment by F_n was removed. To do this, we rearranged eq 7 to solve for ΔC_P given F_n, then varied F_n, to solve for background C_P for both cores and ΔC_P such that carbon-normalized values of $C_{Ppre\text{-}1850,UP}$ and $C_{Ppre\text{-}1850,DN}$ were equal. By this approach, we found that an F_n of 2.6 μg/m^2·year results in an equal carbon-normalized C_P (0.65 μg Hg/g OC) and ΔC_P of 0.016 μg/g ($C_{Ppre\text{-}1850,UP}$ of 0.061 μg/g and $C_{Ppre\text{-}1850,DN}$ of 0.077 μg/g). These C_P concentrations are equivalent to background Hg fluxes from focusing (F_P) of 10 and 3.1 μg/m^2·year at HOB.UP and HOB.DN, respectively. Solving eq 8 and 9 with these values of F_n and ΔC_P yielded estimates of F_a for 1899−2000 (Figure 2e and Supporting Information Table S-5). Modeled Hg fallout is slightly smaller for the first half of the 20th century relative to the FF approaches and larger in the latter half of the century, with the maximum of 20.3 μg/m^2·year at the top of the cores.

The model separates direct fallout flux to the cores from particle-associated flux to the cores, regardless of whether the latter comes from within the lake or from the watershed (F_L and F_W in eq 3). To verify that this is true, we produced hypothetical pairs of core samples by specifying fluxes from each source in eq 3, then solved the DCMB model for fallout using these core samples (see the Supporting Information). This "reverse" modeling approach shows that the DCMB model correctly separates fallout fluxes from sediment-associated fluxes, regardless of whether the latter come from in-lake or watershed sources (Supporting Information Table S-6). Variations in the initial concentration from in-lake (C_{PL}) and watershed (C_{PW}) particle-associated sources also resulted in the correct F_n using DCMB when C_{PL} and C_{PW} were varied in such a way that the original core-interval concentrations resulted. This indicates that the C_P solved for by the model is the average of C_{PL} and C_{PW}. The model fails to return the correct F_n when C_P values for one core are unrelated to C_P values for the other core. This might be the case if, for example, there is a ΔC_P that is not adjusted for or there are markedly different sediment sources to each coring location.

Discussion

Fallout Estimation Methods Using Cores from Hobbs Lake. Here we have used an algebraic solution of mass-balance equations for two cores in a lake to estimate fallout rates. The results compare favorably to those obtained using a more traditional approach based on ^{210}Pb FFs, but both approaches rely on assumptions whose validity will affect estimated fluxes. Both approaches, for example, assume that direct fallout of Hg on a lake surface is incorporated into bottom sediments. This assumption is central to most coring approaches used to estimate fallout, although its validity could vary from one lake to another.

The DCMB approach assumes that particle-associated input concentrations in the two cores are similar or can be adjusted for. The approach also assumes that, on the time scale represented by the core sample intervals (5−15 years), the cores respond simultaneously to changes in contaminant inputs to the lake. The model appears to be quite sensitive to MAR in the cores; large uncertainty in estimation of MARs in the 1800s precluded application of the model to pre-1900 intervals. As demonstrated by the reverse modeling exercise, the DCMB model includes in-lake focusing and watershed inputs in the particle-associated input term (C_P) and correctly handles variations in their relative inputs, but the model fails if C_P in one core is independent of C_P in the other core, or if they are related but the difference (ΔC_P) is not known and not adjusted for. The assumptions of the DCMB model probably apply best to lakes with relatively simple geometries and a single dominant tributary source of sediment, like Hobbs Lake. The model might not work for lakes with spatially variable sedimentation patterns in response to extreme events (*30*), for large lakes with a long delay in fluvial transport in the down-lake direction, or for lakes with fluvial inputs from dissimilar subwatersheds.

The FF_{SC} approach assumes that transport of Hg from the watershed is proportional to transport of ^{210}Pb. However, the geochemistry of Hg and ^{210}Pb are quite different. Reemission of some of the Hg deposited on the watershed, for example, could result in less fluvial transport of Hg to the lake relative to transport of ^{210}Pb, resulting in an underestimation of fallout of Hg on the basis of a ^{210}Pb-based FF_{SC}. This approach also assumes that focusing is constant, which may not adequately describe focusing of a contaminant with a highly variable fallout history. Fluvial input to lakes from historically contaminated soils can continue long after cessation of fallout (*31, 32*). If fallout stopped tomorrow, it might take decades for Hg flux to return to preindustrial levels, as indicated by gradual decreases in ^{137}Cs in lake cores long after fallout ceased (*32*). A portion of that continuing input would be identified mistakenly as fallout.

Using the DCMB model results, we can estimate focusing factors of Hg (FF_{Hg}) to each core by ratio of total Hg accumulation to fallout ($F_n + F_a$). Where DCMB can be applied, this represents an improvement over the FF_{SC} approach because F_a is not assumed to be constant and, therefore, can potentially adjust for delayed inputs from focusing over time. As fallout has increased over the past century, the estimated FF_{Hg} have generally decreased. FF_{Hg} at the tops of the cores are 1.3 and 1.9 for HOB.DN and HOB.UP, compared to pre-1955 mean values of about 2.0 and 4.6. This pattern might reverse when fallout is decreasing, with a trend toward increasing fluvial inputs from residual contamination of the watershed relative to fallout.

Comparison of Lake and Ice Core Fallout Records. Anthropogenic Hg fallout estimates are generally similar for Hobbs Lake and the Upper Fremont Glacier ice core in the 20th century. Fallout in both media was low from about 1900 through the 1930s and, for modern industrial emissions, peaked at 20.3 μg/m^2·year in the 1980s in the ice core (*23*), matching the magnitude of the DCMB model for Hobbs Lake at the top of the cores. There are, however, several notable differences in these fallout records. The ice core Hg peak (early 1980s) is followed by a rapid decline to the mid-1990s when the core was taken. There does not appear to have been a similar decline in Hg emissions regionally or globally (*13, 33*). One possibility is that the retention of Hg deposited on the glacier has changed. Interactions between the atmosphere and Hg deposited in snow are complex; Hg^{2+} deposited in snow is photolabile, and hence to a certain extent it is transformed to Hg^0 and reemitted to the atmosphere (*34*). The period of rapid decrease in Hg deposition in the ice core coincides with a period of rapid temperature increase (~3.5 °C) based on an ^{18}O temperature reconstruction from the same cores (*35*).

Another difference in the two Hg records is that large peaks in Hg deposition from major volcanic eruptions appear

in the ice cores but not in the lake cores. Large volcanic eruptions can distribute dust globally (*36*). Greater particle fallout will cause higher Hg concentration in a layer of ice relative to other layers because there are more particles, even if the particles are no more contaminated than usual. These same dust-fall events normally will not be seen in a lake core because the Hg concentration in volcanic dust is not elevated relative to soils (*37, 38*).

A third difference is that concentration profiles in both lake cores and MAR-FF_{SC} fallout estimates suggest very little fallout during the North American gold rush in the 1850s to 1880s, a period of very large Hg emissions (*13*) and enhanced Hg deposition (4.84 $\mu g/m^2 \cdot$year) in the ice core (*23*). Higher fallout in HOB.DN using a flux-based background correction is suspect because of large uncertainty in MARs in the 1800s. The lack of a gold-rush Hg signal in lake cores has been noted elsewhere (e.g., refs *2 and 13)*. We cannot explain this difference, thus raising yet another interesting question about retention of Hg deposition in lake sediment and ice.

Regional Context of Hg Trends in Hobbs Lake. Increasing atmospheric Hg deposition trends to the present in the north-central Rocky Mountains indicated by the Hobbs Lake cores are part of a pattern of regional differences in Hg trends in North America. Many coring studies have shown recent declines (post-1970s) in Hg deposition, especially in areas experiencing reductions in industrial emissions (e.g., the upper midwest (*20*) and northeastern United States (*8*) and Europe (*39*)). Some cores from remote locations, however, have shown upward trends to the present (e.g., western United States (*40*), Alaska (*2*), and northern Canada (*41*)). Other studies have found a mix of upward and downward trends in the same region (New England (*12*) and Michigan (*16*)). A study of 35 lakes from across the United States found that about half the lakes had no statistically significant trend in Hg concentration since 1970, and that for the lakes with trend, downward trends were twice as likely as upward trends (*7*). Recent work by Landers et al. (*42*) shows both upward and downward Hg trends in lake cores from national parks in the western United States and Alaska, including upward trends in cores from lakes in Glacier and Mount Rainier National Parks with focus-corrected fluxes (13−18 $\mu g/m^2 \cdot$year) similar to Hobbs Lake fallout estimates. Although the details are not entirely clear, it seems reasonable to conclude that continuing increases in Hg deposition are more common in western North America and the Arctic than in eastern North America and Europe.

Global and regional Hg emissions appear to be affecting Hg trends at Hobbs Lake. The average rate of increase in Hg fallout at Hobbs Lake since 1980 is 2.3% per year using the DCMB model and 1.9% using the MAR-FF_{SC} approach, comparable to the reported a 2% per year rate of increase in global emissions from 1982 to 1991 (*13*). Unlike the eastern United States, Hg emissions in the western United States have not decreased in recent years (*33*). Two regional sources of Hg in the west that are much less important in the east are mining (U.S. EPA Toxic Release Inventory, http://www.epa.gov/tri/) and forest fires (*43*).

Finally, there are likely large variations in Hg fallout in the west because of large variations in precipitation and elevation. Increased Hg deposition with elevation is expected because of increased precipitation, decreased temperatures, and because of high concentrations of reactive gaseous mercury in the troposphere from oxidation of gaseous elemental mercury (*44*). Recent Hg fallout estimates to Hobbs Lake (16−20 $\mu g/m^2 \cdot$year) are about 4 times higher than measured wet deposition at a site in northwestern Wyoming (mercury deposition network (MDN) site WY08, http://nadp.sws.uiuc.edu/mdn/). The MDN site, however, is at lower elevation (1912 m) and only measures wet deposition, whereas the lake captures wet and dry deposition. This suggests that Hg fallout estimated from high-elevation lake and ice cores may not be representative of fallout for lower elevations in the western United States.

Acknowledgments

We thank the reviewers for their time and many helpful and insightful comments. We also thank Ted Porwoll of the National Forest Service for assistance with sampling and providing background information on the lake.

Supporting Information Available

Additional figures and tables and an evaluation of the validity of the DCMB model. This material is available free of charge via the Internet at http://pubs.acs.org.

Literature Cited

(1) Landers, D. H.; Gubala, C. P.; Verta, M.; Lucotte, M.; Johansson, K.; Vlasova, T.; Lockhard, W. L. Using lake sediment mercury flux ratios to evaluate the regional an dcontinental dimensions of mercury deposition in Arctic and Boreal ecosystems. *Atmos. Environ.* **1998**, *32* (5), 919–928.

(2) Fitzgerald, W. F.; Engstrom, D. R.; Lamborg, C. H.; Tseng, C.-M.; Balcom, P. H.; Hammerschmidt, C. R. Modern and historic atmospheric fluxes in Northern Alaska: Global sources and arctic depletion. *Environ. Sci. Technol.* **2005**, *39* (2), 557–568.

(3) Lindberg, S.; Bullock, R.; Ebinghaus, R.; Engstrom, D. R.; Feng, X.; Fitzgerald, W. F.; Pirrone, N.; Prestbo, E.; Seigneur, C. A systhesis of progress and uncertainties in attributing the sources of mercury in deposition. *Ambio* **2007**, *36* (1), 19–32.

(4) Jackson, T. A. Long-range atmospheric transport of mercury to ecosystems, and the importance of anthopogenic emissions—a critical review and evaluation of the published evidence. *Environ. Rev.* **1997**, *5* (2), 99–120.

(5) Swain, E. B.; Engstrom, D. R.; Brigham, M. E.; Henning, T. A.; Brezonik, P. L. Increasing rates of atmospheric mercury deposition in Midcontinental North America. *Science* **1992**, *257* (5071), 784–787.

(6) Renberg, I.; Brännvall, M.-L.; Richard, B.; Ove, E. Atmospheric lead pollution history during four millennia (2000 BC to 2000 AD) in Sweden. *Ambio* **2000**, *29* (3), 150–156.

(7) Mahler, B. J.; Van Metre, P. C.; Callender, E. Trends in metals in urban and reference lake sediments across the United States, 1975−2001. *Environ. Toxicol. Chem.* **2006**, *25* (7), 1698–1709.

(8) Kamman, N. C.; Engstrom, D. R. Historical and present fluxes of mercury to Vermont and New Hampshire lakes inferred from 210Pb dated sediment cores. *Atmos. Environ.* **2002**, *36*, 1599–1609.

(9) Likens, G. E.; Davis, M. B. Post-glacial history of Mirror Lake and its watershed in New Hampshire, U.S.A.: An initial report. *Int. Ver. Theor. Angew. Limnol., Verh.* **1975**, *19*, 982–993.

(10) Hilton, J. A conceptual framework for predicting the occurrence of sediment focusing and sediment redistribution in small lakes. *Limnol. Oceanogr.* **1985**, *30* (6), 1131–1143.

(11) Van Metre, P. C.; Callender, E.; Fuller, C. C. Historical trends in organochlorine compounds in river basins identified using sediment cores from reservoirs. *Environ. Sci. Technol.* **1997**, *31* (8), 2339–2344.

(12) Perry, E.; Norton, S. A.; Kamman, N. C.; Lorey, P. M.; Driscoll, C. T. Deconstruction of historic mercury accumulation in lake sediments, Northeastern United States. *Ecotoxicology* **2005**, *14*, 85–99.

(13) Pirrone, N.; Allegrini, I.; Keeler, G. J.; Nriagu, J. O.; Rossmass, R.; Robbins, J. A. Historical atmospheric mercury emissions and depositions in North America compared to mercury accumulations in sedimentary records. *Atmos. Environ.* **1998**, *32* (5), 929–940.

(14) Lamborg, C. H.; Fitzgerald, W. F.; Damman, A. W. H.; Benoit, J. M.; Balcom, P. H.; Engstrom, D. R. Modern and historic atmospheric mercury fluxes in both hemispheres: Global and regional mercury cycling implications. *Global Biogeochem. Cycles* **2002**, *16* (4), 1104–1115.

(15) Chalmers, A. T.; Van Metre, P. C.; Callender, E. The chemical response of particle-associated contaminants in aquatic sediments to urbanization in New England, U.S.A. *J. Contam. Hydrol.* **2007**, *91*, 4–25.

(16) Parsons, M. J.; Long, D. T.; Yohn, S. S.; Giesy, J. P. Spatial and temporal trends of mercury loadings to Michigan inland lakes. *Environ. Sci. Technol.* **2007**, *41*, 5634–5640.

(17) Krabbenhoft, D. P.; Benoit, J. M.; Babiarz, C. L.; Hurley, J. P.; Andren, A. W. Mercury cycling in the Allequash Creek watershed, Northern Wisconsin. *Water, Air, Soil Pollut.* **1995**, *80*, 425–433.
(18) Appleby, P. G.; Oldfield, F. Application of lead-210 to sedimentation studies. In *Uranium-Series Disequilibrium: Applications to Earth, Marine, and Environmental Sciences*, 2nd ed.; Ivanovich, M., Harmon, S., Eds.; Clarendon Press: Oxford, U.K., 1992; p 910.
(19) Eisenreich, S. J.; Capel, P. D.; Robbins, J. A.; Boubonniere, R. A. Accumulation and diagenesis of chlorinated hydrocarbons in lacustrine sediments. *Environ. Sci. Technol.* **1989**, *23* (9), 1116–1126.
(20) Engstrom, D. R.; Swain, E. B. Recent declines in atmospheric mercury deposition in the Upper Midwest. *Environ. Sci. Technol.* **1997**, *31* (4), 960–967.
(21) Balogh, S. J.; Engstrom, D. R.; Almendinger, J. E.; Meyer, M. L.; Johnson, D. K. History of mercury loading in the Upper Mississippi River reconstructed from the sediments of Lake Pepin. *Environ. Sci. Technol.* **1999**, *33* (19), 3297–3302.
(22) Van Metre, P. C.; Mahler, B. J. Contaminant trends in reservoir sediment cores as records of influent stream quality. *Environ. Sci. Technol.* **2004**, *38* (11), 2978–2986.
(23) Schuster, P. F.; Krabbenhoft, D. P.; Naftz, D. L.; Cecil, L. D.; Olson, M. L.; Dewild, J. F.; Susong, D. D.; Green, J. R.; Abbott, M. L. Atmospheric mercury deposition during the last 270 years: A glacial ice core record of natural and anthropogenic sources. *Environ. Sci. Technol.* **2002**, *36* (11), 2303–2310.
(24) Van Metre, P. C.; Wilson, J. T.; Fuller, C. C.; Callender, E.; Mahler, B. J. Methods, site characteristics, and age dating of sediment cores for 56 U.S. lakes and reservoirs sampled by the USGS National Water-Quality Assessment Program, 1993−2001; SIR 2004-5184; U.S. Geological Survey: Denver, CO, 2004; p 120.
(25) Fuller, C. C.; van Geen, A.; Baskaran, M.; Anima, R. Sediment chronology in San Francisco Bay, California, defined by 210Pb, 234Th, 137Cs, and 239, 240Pu. *Mar. Chem.* **1999**, *64*, 7–27.
(26) Arbogast, B. F. E. Analytical methods manual for the Mineral Resource Surveys Program, U.S. Geological Survey. *Open-File Rep.—U.S. Geol. Surv.* **1996**, *96-0525*, 10.
(27) Binford, M. W. Calculation and uncertainty analysis of 210Pb dates for PIRLA project lake sediment cores. *J. Paleolimnol.* **1990**, *3*, 253–267.
(28) Carario, J.; Vale, C.; Nogueira, M. The pathway of mercury in contaminated waters determined by association with organic carbon (Tagus Estuary, Portugal). *Appl. Geochem.* **2008**, *23*, 519–528.
(29) Horowitz, A. J. *A Primer on Sediment-Trace Element Chemistry*, 2nd ed.; Lewis Publishing Company: Chelsea, MI, 1991.
(30) Schiefer, E. Depositional regimes and areal continuity of sedimentation in a montane lake basin, British Columbia, Canada. *J. Paleolimnol.* **2006**, *35*, 617–628.
(31) Yang, H.; Rose, N. L.; Battarbee, R. W.; Boyle, J. F. Mercury and lead budgets for Lochnagar, a Scottish mountain lake and its catchment. *Environ. Sci. Technol.* **2002**, *36* (7), 1383–1388.
(32) Van Metre, P. C.; Wilson, J. T.; Callender, E.; Fuller, C. C. Similar rates of decrease of persistent, hydrophobic contaminants in riverine systems. *Environ. Sci. Technol.* **1998**, *32* (21), 3312–3317.
(33) Butler, T. J.; Cohen, M. D.; Vermeylen, F. M.; Likens, G. E.; Schmeltz, D.; Artz, R. S. Regional precipitation mercury trends in the eastern USA, 1998−2005: Declines in the Northeast and Midwest, no trend in the Southeast. *Atmos. Environ.* **2008**, *42*, 1582–1592.
(34) Lalonde, J. D.; Poulain, A. J.; Amyot, M. The role of mercury redox reactions in snow on snow-to-air mercury transfer. *Environ. Sci. Technol.* **2002**, *36* (2), 174–178.
(35) Naftz, D. L.; Susong, D. D.; Schuster, P. F.; Cecil, L. D.; Dettinger, M. D.; Michel, R. L.; Kendall, C. Ice core evidence of rapid air temperature increases since 1960 in alpine areas of the Wind River Range, Wyoming, United States. *J. Geophys. Res.* **2002**, *107* (D13), 4171.
(36) Lamb, H. H. Volcanic dust in the atmosphere: with a chronology and assessment of its meteorological significance. *Philos. Trans. R. Soc. London* **1970**, *266*, 425–533.
(37) Smichowski, P.; Gomez, D.; Rosa, S.; Polla, G. Trace elements content in size-classified volcanic ashes as determined by inductively coupled plasma-mass spectrometry. *Microchem. J.* **2003**, *75* (2), 109–117.
(38) Tomiyasu, T.; Okada, M.; Imura, R.; Sakamoto, H. Vertical variations in the concentration of mercury in soils around Sakurajima Volcano, Southern Kyushu, Japan. *Sci. Total Environ.* **2003**, *304* (1−3), 221–230.
(39) Bindler, R. Estimating the natural background atmospheric deposition rate of mercury utilizing ombrotrophic bogs in Southern Sweden. *Environ. Sci. Technol.* **2003**, *37*, 40–46.
(40) Sanders, R. D.; Caoale, K. H.; Gill, G. A.; Andrews, A. H.; Stephenson, M. Recent increase in atmospheric deposition of mercury to California aquatic systems inferred from a 300-year geochronological assessment of lake sediments. *Appl. Geochem.* **2008**, *23*, 399–407.
(41) Lockhard, W. L.; Wilkinson, P.; Billeck, B. N.; Hunt, R. V.; Wagemann, R.; Brunskill, G. J. Current and historical inputs of mercury to high-latitude lakes in Canada and to Hudson Bay. *Water, Air, Soil Pollut.* **1995**, *80* (1−4), 603–610.
(42) Landers, D. H.; Simonich, D. A.; Jaffe, L. H.; Geiser, D. H.; Campbell, D. H.; Schwindt, C. B.; Schreck, M. L.; Kent, W. D.; Havner, H. E.; Taylor, K. J.; Hageman, S.; Usenko, L. K.; Ackerman, J. E.; Schrlau, N. L.; Rose, N. L.; Blett, T. R.; Erway, M. M. The fate, transport, and ecological impacts of airborne contaminants in Western National Parks (USA); U.S. Environmental Protection Agency, Office of Research and Development, Western Ecolory Division: Corvallis, OR, 2008.
(43) Wiedinmyer, C.; Friedli, H. Mercury emission estimates from fires: An initial inventory for the United States. *Environ. Sci. Technol.* **2007**, *41* (23), 8092–8098.
(44) Swartzendruber, P. C.; Jaffe, D. A.; Prestbo, E. M.; Weiss-Penzias, P.; Selin, N. E.; Park, R.; Jacob, D. J.; Strode, S.; Jaegle, L. Observations of reactive gaseous mercury in the free troposphere at the Mount Bachelor Observatory. *J. Geophys. Res.* **2006**, *111*, D24301.

ES801490C